





Article

Chironomid-Based Modern Summer Temperature Data Set and Inference Model for the Northwest European Part of Russia

Larisa Nazarova ^{1,2,*} , Liudmila Syrykh ^{2,3} , Ivan Grekov ², Tatiana Sapelko ⁴ , Andrey B. Krasheninnikov ⁵ 
and Nadia Solovieva ^{6,7}

- ¹ Alfred Wegener Institute, Helmholtz Centre for Polar and Marine Research, Research Unit Potsdam, Telegrafenberg A43, 14473 Potsdam, Germany
- ² Faculty of Geography, Herzen State Pedagogical University of Russia, Moika 48, 191186 St. Petersburg, Russia
- ³ Laboratory of Paleoclimatology, Paleoecology, Paleomagnetism, Kazan Federal University, 420018 Kazan, Russia
- ⁴ Institute of Limnology of the Russian Academy of Sciences—SPC RAS, 195106 St. Petersburg, Russia
- ⁵ Institute of Biological Problems of the North, FEB RAS, 685000 Magadan, Russia
- ⁶ Environmental Change Research Centre, Department of Geography, University College London, London WC1E 6BT, UK
- ⁷ General Studies Division, Higher Colleges of Technology, Sharjah 61174, United Arab Emirates
- * Correspondence: nazarova_larisa@mail.ru

Abstract: Northwestern Russia remains the only region in Northern Eurasia where no regional chironomid-based inference model for quantitative palaeoclimatic reconstructions has been developed. Using palaeolimnological methods, we investigated the subfossil chironomid remains in surface sediments from a data set of 98 lakes from nine subregions of the European part of Northern Russia. We identified 143 chironomid taxa in the investigated lakes. Multivariate statistical analyses of chironomid and environmental data demonstrated that the mean July air temperature (T July), distance from the tree line, water depth, pH, and altitude explain the most significant variance in chironomid distribution. T July appeared to be the most important environmental variable. We established a chironomid-based inference model for reconstructing T July from subfossil data. The resulting West Russian two-component WA-PLS model includes 96 lakes (two lakes were excluded as outliers), 143 chironomid taxa, $r^2 = 0.84$ (r^2 boot = 0.60), RMSEP boot = 1.34 °C, and can be recommended for application in palaeoclimatic studies in the East of Northern Eurasia.

Keywords: chironomids; database; T July; inference model; lakes; sediments; northwest Russia



Citation: Nazarova, L.; Syrykh, L.; Grekov, I.; Sapelko, T.; Krasheninnikov, A.B.; Solovieva, N. Chironomid-Based Modern Summer Temperature Data Set and Inference Model for the Northwest European Part of Russia. *Water* **2023**, *15*, 976. <https://doi.org/10.3390/w15050976>

Academic Editor: José Luis Sánchez-Lizaso

Received: 3 January 2023
Revised: 23 February 2023
Accepted: 28 February 2023
Published: 3 March 2023



Copyright: © 2023 by the authors. Licensee MDPI, Basel, Switzerland. This article is an open access article distributed under the terms and conditions of the Creative Commons Attribution (CC BY) license (<https://creativecommons.org/licenses/by/4.0/>).

1. Introduction

Chironomids (Insecta: Diptera: Chironomidae), or non-biting midges, are holometabolous insects. Their aquatic larvae usually constitute the most abundant macroinvertebrate benthic group in freshwaters [1,2]. They are critical, primary consumers that play an essential role in the biogeochemical cycling of nutrients in lake ecosystems [3,4]. Chironomids are diverse and nearly ubiquitous. Many studies prove that the abundance and distribution of most chironomid taxa are temperature-dependent [5–8]. They respond rapidly to climate change by virtue of the winged adult stage. The larval head capsules preserve well in lake sediment deposits, and the subfossils are identifiable in most cases to at least the genus morphotype [5]. Due to these features, chironomids have been proven to be among the most reliable quantitative proxies of mean July air temperature [4–7]. Climatic reconstructions from palaeorecords are based on modern analogues (training sets) from which the inference models or transfer function can be established. Past climates can be quantified from fossil chironomid assemblages by using inference models that tie the distribution and abundance of chironomids to the contemporary climate [4–6].

Datasets describe the relationship between modern chironomid assemblages and environmental conditions (predominantly the mean July air temperature (T July)). Based on these datasets, inference models for reconstructing T July have been developed successfully all over the world [9–11]. There are several datasets and chironomid-based inference models for reconstructing the T July in Northern Europe [12–16]. Our previous studies on the distribution and abundance of chironomids in lakes along environmental gradients in north-eastern Eurasia encompass many regions, including the Polar Urals, Siberia, and Kamchatka [16–20]. These modern chironomid-based training sets were used for the development of region-quantitative transfer functions for reconstructing T July, water depth (WD), and continentality (CI) [16,18,19].

However, chironomid distribution in relation to environmental factors in modern lake sediments in the northern regions of east Europe (northwestern Russia) has never been investigated [21,22] apart from case studies in the Bolshezemelskaya tundra and Pechora River basin (northwest of the Polar Urals) [23–25].

Since chironomid-based inference models can hardly be used outside of the regions in which they were developed [26–29], it was imperative to develop a regional chironomid-based inference model for application in the east European North. For this reason, the main goal of our investigation is to fill in this gap in chironomid studies in northern Eurasia.

In this paper, we present the results of our work in reanalysing and standardising the taxonomy between our earlier published data from two regions in the west European part of the Russian arctic (Pechora and Komi, Figure 1; [16,19,23]) and the addition of new sampling regions to the data set: Anzher Solovki (seven lakes), the central European region (three lakes), Karelian Isthmus and Ladoga (twenty-three lakes), the Kola Peninsula (nine lakes), Karelia Zaonezhje (twelve lakes), Novaya Zemlya (one lake), and the Onega Peninsula (six lakes) (Figure 1). Following taxonomic standardisation and the analysis of taxonomic distances between the sampling regions, we merged the data sets. Merging the datasets has essential advantages, including extending the environmental and geographical gradients, increasing the representation of taxa in the calibration set, improving the performance, and widening the applicability of the chironomid–temperature inference model by providing more reliable estimates of the environmental optima of chironomid taxa [5,23]. The inclusion of a greater number of the geographically and ecologically suitable lakes into the model increases the probability of better analogues between present and past assemblages [5].

The main objectives of our investigation are to compare the faunal composition of the previously studied and newly sampled parts of the data set to examine the influence of environmental factors on chironomid distribution and abundance in the “chironomid-environment” dataset of the lakes in northwestern Russia and to produce a chironomid-based regional inference model for reconstructing past regional climate and environmental changes in the north of eastern Europe.

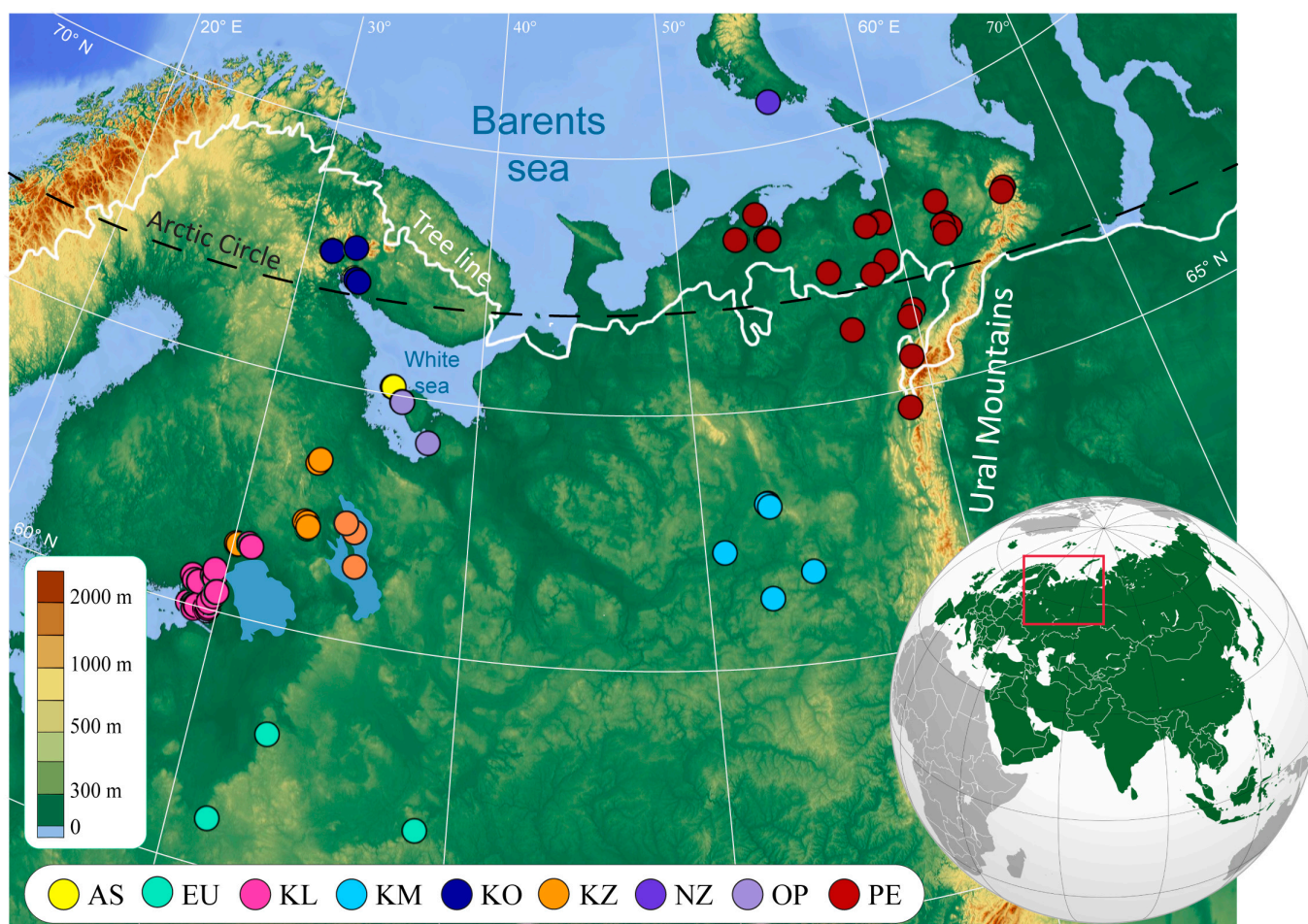


Figure 1. Location of the lakes in the sampling regions: Anzher Solovki (AS); central European region (EU), Karelian Isthmus, Ladoga (KL); Komi (KM, [19]); Kola Peninsula (KO); Karelia Zaonezhje (KZ); Novaya Zemlya (NZ); Onega Peninsula (OP); and Pechora (PE, [19]). Relief map and tree line have been taken from free online sources: <https://maps-for-free.com>; <http://ecoregions.appspot.com> (accessed on 27 February 2023).

2. Materials and Methods

2.1. Field Methods and Derivation of Climate Variables

Surface sediment samples and environmental data were collected between 2015 and 2020 in several regions of north European Russia. They were supplemented by the data collected earlier in the north-eastern part of European Russia (Komi and Pechora region) that were used in the previously published North Russian data set and inference models [19] (Figure 1). The data set included 98 lakes that are situated across wide latitudinal and longitudinal ranges and several environmental zones (arctic desert, tundra, forest tundra, northern taiga, and taiga) (Table 1).

The sediment samples were collected from the deepest point of each lake using a 60 mm diameter UWITEC gravity corer or an 80 mm diameter HON-Kajak corer [30] and a Voronkov lot. The water depth (WD) was measured using an echolot. The pH was measured using a multi-parameter instrument (WTW 330 i, 340 i). The mean July temperature (T July) for each site was obtained from a climatic data set compiled by New et al. [31] with a 10 min latitude/longitude resolution. Though this data set has some shortfalls (including a relatively coarse resolution of the climate data; that the climate normals predate the collection of the chironomid data; and that the data span a cold phase of the Arctic Oscillation) [32], its global nature, homogeneity and consistency make it suitable for our investigation. In most cases, the data from local meteorological stations have gaps in

their observations and cover different time spans. The distance from the tree line (DTL) was calculated using the treeline location [33] in ArcGIS [34].

Table 1. Summary of environmental data for the 98 lakes. St.dev for standard deviation; skew for skewness.

Parameters *	Min.	Max.	Mean	Median	St.dev	Skew
Latitude, N	56.22	70.59	64.17	64.89	3.22	−0.26
Longitude, E	28.85	66.32	42.05	36.03	12.77	0.50
Altitude, m a.s.l.	0	514	74.30	60.00	71.02	2.76
T July °C	9.20	18.10	15.04	15.1	1.97	−0.51
Water depth, m	0.70	140	9.74	5.7	16.39	5.88
pH	4.54	9.5	6.72	6.8	0.86	−0.05
Distance from treeline, km	−1434	356	−390.42	−275	403.29	−0.35
Water depth, log 10	−0.15	2.15	0.77	0.76	0.40	0.59
Altitude, log 10	0.18	2.71	1.67	1.78	0.50	−0.66

* Vegetation types include: arctic desert; tundra; forest tundra; northern taiga; and taiga. They are presented in more detail in the Supplementary electronic material, Table S1.

2.2. Chironomid Analysis

The treatment of the sediment samples for chironomid analysis followed the standard techniques described in [27]. Chironomids were identified to the highest taxonomic resolution possible with reference to [27,35]. At least 50 head capsules (HC) were extracted from each sample to reach the diversity of the chironomid population sufficient to accurately estimate the inferred temperature [36,37].

2.3. Numerical Methods

The dataset of 98 lakes was analysed to examine the relationship between chironomid distribution and abundance and the environmental variables. All taxon data were transformed to percent abundances, calculated as the percentage of total identifiable chironomids per sample. They were square root transformed prior to analysis [9,38]. Environmental variables were controlled for skewness [39]. Significantly skewed data, values of which exceeded two standard errors of skewness (regardless of sign) [40], were log transformed (Altitude and WD). The remaining parameters were left untransformed.

A detrended correspondence analysis (DCA) with detrending by segments (rare taxa downweighted) was performed on the chironomid data to explore the main pattern of taxonomic variation between the investigated lakes and to determine the lengths of the sampled environmental gradients [41,42]. Results of the DCA showed that the gradient length of species scores for the axes 1 and 2 were 4.075 and 4.334 standard deviation units, respectively, indicating that numerical methods based on a unimodal response model were the most relevant for assessing the variation of the chironomid assemblages [43–45].

Variance inflation factors (VIF) were used to identify intercorrelated variables. Environmental variables with a VIF greater than 20 were eliminated, starting with the variable with the largest inflation factor and continuing until all remaining variables had values <20 [46]. We investigated the relationships between the significant environmental variables and the individual axes by using correlation coefficients, t-values, and interest correlations [19,46]. The relationships between chironomid distribution and environmental variables were assessed by canonical correspondence analyses (CCA), using each environmental variable as the sole constraining variable. The statistical significance of each variable was tested using a Monte Carlo permutation test with 999 unrestricted permutations [47]. Significant variables ($p \leq 0.05$) were retained for further analysis. Both the DCA and CCA were performed using CANOCO 4.5 [48].

Taxonomic similarities between the investigated regions within the data set were estimated using DCA, and the squared-chord distance was used as a measure of taxonomic

distances [49] had performed in the program PAST [50]. The TD values ranged from 0 to 2, with 0 indicating an identical taxonomic composition of the samples [51].

2.4. Model Development

We used the environmental variable that explained the most variance in the data set (as indicated by the CCAs) in order to develop quantitative transfer functions based on weighted averaging partial least squares (WA-PLS) methods [15,19,52,53]. Relationships between the significant environmental variables and the individual CCA axes in the models were tested with *t*-values, correlation coefficients, and intersite correlations. The critical value for a *t*-test is 2.1 at the 5% significance level [46].

The performance and optimal number of components in the transfer functions were assessed using bootstrapping cross validation. The resulting inference models were examined by means of the coefficient of determination (r^2_{boot}), root mean squared error of prediction (RMSEP), [54] and the max bias_{boot} (the tendency of the model to under- or overestimate the reconstructed parameter). The development of the transfer function aims at a high coefficient of determination (r^2_{boot}), a low RMSEP, and low mean and maximum bias_{boot} [55]. To improve the quality of the transfer function, we deleted several lakes from the analysis. These lakes were defined as outliers based on their absolute residual of the samples that exceeded the standard deviation of T July in all models [56].

Optima and tolerances for all chironomid taxa retained in the analyses were estimated by weighted averages and weighted standard deviations [57]. The program C2, version 1.7.7, was used to develop transfer functions and to estimate N2 as a measure of the frequency of occurrence of the taxa in the data set, optima, and tolerances [58,59].

To describe the relationship of chironomid taxa to the main environmental variable, taxon response models were generated using generalized linear models (GLM) and set to a quadratic degree and Poisson distribution ($p < 0.05$, significant; $p < 0.001$ highly significant) in the CanoDraw component of CANOCO 4.5 [18,19,46].

3. Results

3.1. Environmental Parameters of the Lakes

The range of the available environmental parameters common for all lakes in the dataset is presented in Table 1. The lakes in the West Russian set have an unskewed distribution along the T July, pH, DTL, and parameters of geographical location (latitude and longitude). The WD and altitude (Alt) have a skewed distribution and were log10 transformed. The lakes cover the T July gradient from 9.2 to 18.1 °C. Most of the lakes are located within the T July range of 11.6 to 17.5 °C (Figure 2). The coldest lakes (9.2 to 11.6 °C) are from the Polar Urals and Novaya Zemlya Yuzhny Island (NZ). There are only four lakes deeper than 30 m (*ca* median \pm st. dev): two lakes from the Polar Urals and two lakes from the Ladoga region (Figure 1). Three lakes from the central European part of Russia have the longest DTL to the south. The lake from the NZ is situated the furthest away from the tree line to the north. There are four lakes with a pH above 8; 3 of them are from the Komi region, and one is from the Karelian Isthmus (Malaya Ladoga). Sixteen lakes have a pH below 6 (median \pm st. dev.) and are from different regions.

3.2. Chironomid Fauna

The DCA (Figure 3) and TD (Table 2) analyses demonstrated that NZ is the most taxonomically distinct region and has the closest similarity to Karelian Isthmus. The taxonomical distinction of NZ and Karelian Isthmus is reflected in the DCA biplot, where the lakes are placed as a group at the left side of the diagram (Figure 3). The taxonomically closest regions (the lowest TD) are those in the middle of the DCA plot (Figure 3). These are the geographically close regions: Zaonezhje, Anzher Solovki, and the Onega Peninsula. Other taxonomically close regions are those in the right part of the DCA: Kola and Pechora (Figures 1 and 3, Table 2). The median TD of all the investigated regions is 1.02.

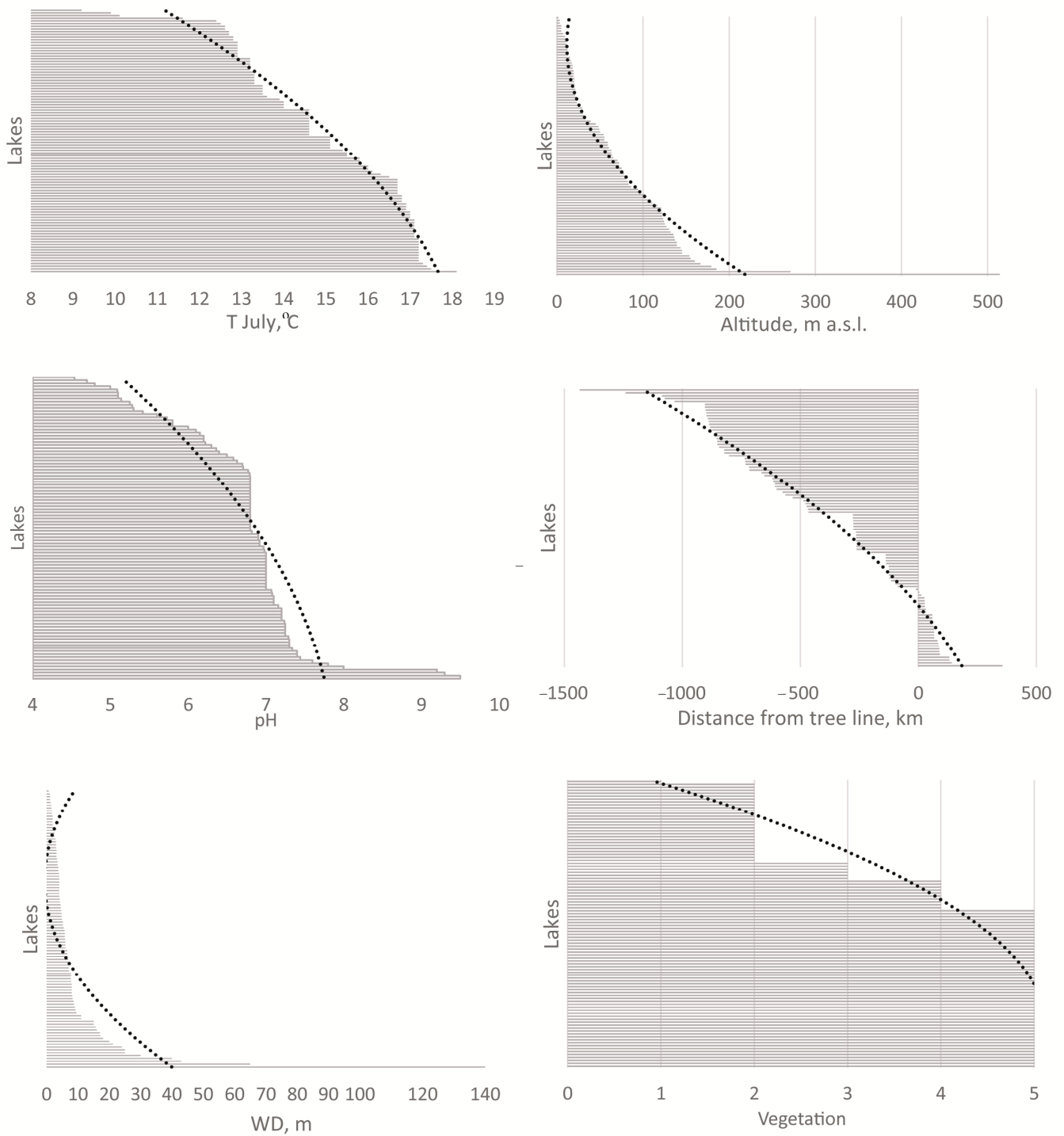


Figure 2. Distribution of the investigated lakes along the environmental gradients. Each horizontal line is a lake. Dashed lines are second-degree polynomial trend lines. Vegetation: one for arctic desert; two for tundra; three for forest tundra; four for northern taiga; and five for taiga.

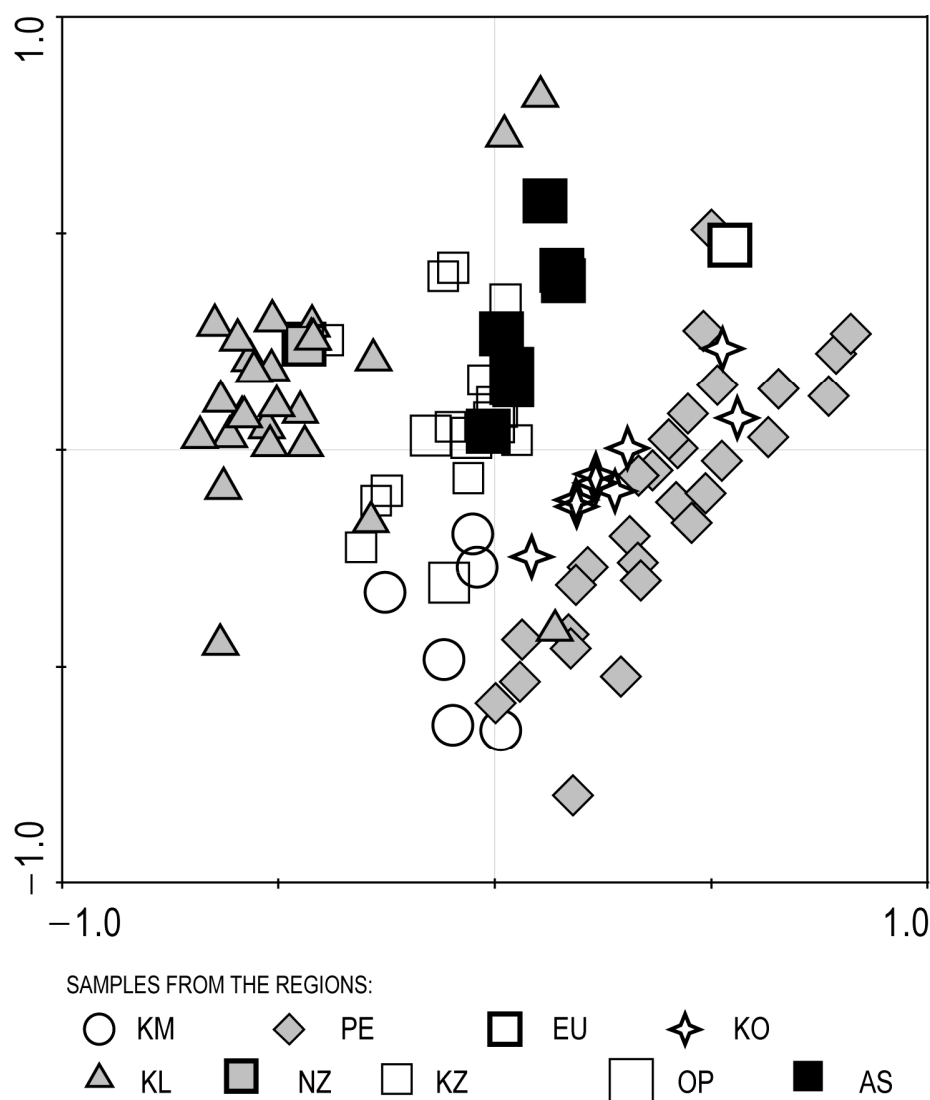


Figure 3. DCA of the lakes with respect to regions of their location based on the taxonomic composition of chironomid fauna. Regions (Abbreviations): Anzher Solovki (AS); central European region (EU), Karelian Isthmus, Ladoga (KL); Komi (KM); Kola Peninsula (KO); Karelia Zaonezhje (KZ); Novaya Zemlya (NZ); Onega Peninsula (OP); and Pechora (PE).

Table 2. Taxonomic distances (TD) between regions of investigations within the data set. Regions are sorted from north to south. Regions (Abbreviations): Novaya Zemlya (NZ); Komi (KM); Kola Peninsula (KO); Anzher Solovki (AS); Onega Peninsula (OP); Pechora (PE); Karelia Zaonezhje (KZ); Karelian Isthmus, Ladoga (KL); and the central European region (EU).

Lake	NZ	KM	KO	AS	OP	PE	KZ	KL	EU	Median
NZ	0	1.39	1.38	1.37	1.38	1.35	1.35	1.28	1.38	1.37
KM	1.39	0	1.06	1.00	0.87	1.02	1.03	1.04	1.20	1.03
KP	1.38	1.06	0	0.94	0.77	0.85	0.96	0.84	1.28	0.94
AS	1.37	1.00	0.94	0	0.70	1.06	1.00	1.06	1.30	1.01
OP	1.38	0.87	0.77	0.70	0	0.98	1.03	0.95	1.28	0.95
PE	1.35	1.02	0.85	1.06	0.98	0	0.90	0.95	1.20	0.98
KZ	1.35	1.03	0.96	1.00	1.03	0.90	0	0.88	1.06	1.01
KL	1.28	1.04	0.84	1.06	0.95	0.95	0.88	0	1.18	0.96
EU	1.38	1.20	1.28	1.30	1.28	1.20	1.06	1.18	0	1.20
Median	1.37	1.03	0.94	1.01	0.95	0.98	1.01	0.96	1.20	1.02

In the 98 investigated lakes from northwest European Russia (new), we identified 143 chironomid taxa. The most common taxa, which were found in more than 50% (≥ 49) of the lakes, are *Psectrocladius sordidellus*-type, *Procladius*, *Cladotanytarsus mancus*-type, *Tanytarsus pallidicornis*-type, *Tanytarsus mendax*-type, *Sergentia coracina*-type, *Microtendipes pedellus*-type, *Dicrotendipes nervosus*-type, *Polypedilum nubeculosum*-type, *Cladopelma lateralis*-type, and *Tanytarsus lugens*-type (Figure 4). The distribution of *Oliveridia*, *Hydrobaenus lugubris*-type, *Smittia*—*Parasmittia*, *Toetenia bavarica*-type, and *Diplocaldius* (rare) is restricted to the coldest lakes in our data set (9–10.5 °C; Figure 4). *Nanocladius rectinervis*-type, *Paralauterborniella*, the *Nanocladius branchicolus*-type, which is rare in the dataset, *Einfeldia dissidens*-type, *Harnischia*, *Nilothauma*, and *Orthocladius* type I (not in Figure 4) are restricted to the lakes from the warmest part of the temperature gradient (16–18.5 °C).

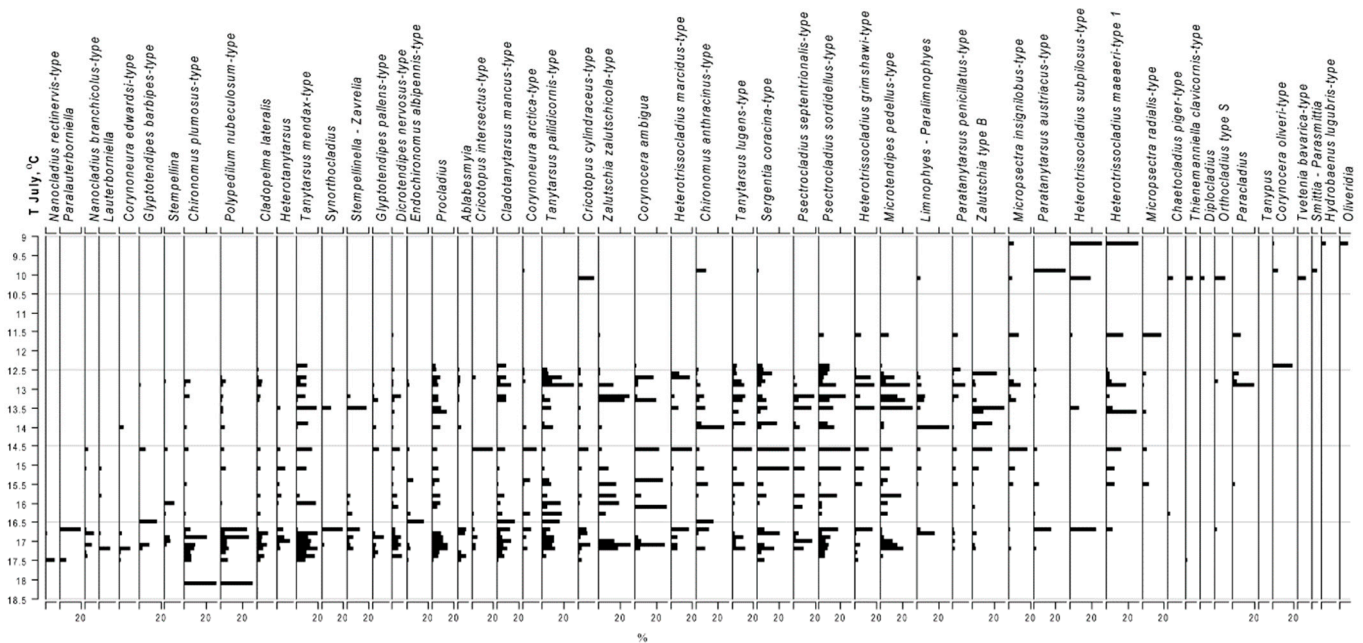


Figure 4. Chironomid taxa in the data set ordered by T July with the warmest at the bottom and the coldest lake at the top. Rare taxa are not included into the diagram. WD is for water depth.

3.3. Ordination of the Set of Data

A CCA with all environmental variables included in the analysis resulted in the parameters presented in Table 3. VIFs from the CCAs show that the latitude and DTL are intercorrelated. The latitude was eliminated from the analysis as having the greatest VIF. A series of CCAs constrained to individual environmental variables and Monte Carlo permutation tests (under full model) revealed that T July, WD, pH, DTL, and altitude explain significant proportions ($p < 0.05$) of variance in the data set. A CCA with five variables had a CCA eigenvalue of axis 1 of 0.154 and a CCA axis 2 of 0.086, explaining 4.7% and 2.6% of the variance in the data, respectively (SEM, Table S2). The ratio of eigenvalues of the CCA axes 1 and 2 in our study is 1.79 ($\lambda_1/\lambda_2 = 0.154/0.086$). This indicates that the most important explanatory variables are most likely included in the analysis [60]. The results of the forward selection suggest (Table 3) that the mean July air temperature was the most significant variable in explaining chironomid distribution in NWE.

Axis 1 of CCA correlates with T July, and CCA axis 2 correlates with DTL (Table 4). The absolute values of canonical coefficients are the highest, and their t -values are greater than 2.1, the critical value for a t -test at the 5% significance level [46]. WD has the strongest correlation with Axis 3. The pH correlates with Axis 4, and Alt demonstrates a correlation with axes 2 and 4. From the obtained results, we can conclude that T July explains the most significant part of the data variance and can be used to develop an inference model.

Table 3. Significant environmental variables identified by forward selection in CCA of 98 lakes NWE data set and the variance they explain.

Variable	Variance Explained	% Total Variance Explained	F Value	Significance Leve
Mean July air temperature (T July)	0.155	38.5	4.069	0.002
Water depth (log 10)	0.092	22.8	2.480	0.002
Distance from tree line	0.084	20.8	2.294	0.002
pH	0.062	15.4	1.969	0.002
Altitude	0.010	2.5	1.700	0.008
Total variance explained	0.403			
Total variance	3.293			

Table 4. Environmental variables, canonical coefficients and t-values of significant environmental variables used in the CCA.

Parameters	Canonical Coefficients				t-Values				Interset Correlation			
	Axis 1	Axis 2	Axis 3	Axis 4	Axis 1	Axis 2	Axis 3	Axis 4	Axis 1	Axis 2	Axis 3	Axis 4
T July	−0.41	−0.03	−0.39	−0.23	−5.31	−0.46	−6.38	−3.53	−0.73	−0.02	−0.32	−0.07
DTL	0.39	−0.42	−0.32	−0.20	5.29	−5.35	−5.18	−2.97	−0.18	0.76	0.22	−0.03
WD	0.16	0.18	−0.20	−0.02	5.17	5.45	−7.76	−0.81	0.18	0.46	−0.53	0.003
pH	0.02	−0.11	0.08	0.24	0.55	−3.26	−2.96	7.97	−0.001	−0.24	−0.30	0.55
Alt	0.01	−0.13	−0.05	−0.11	0.35	−3.89	−2.05	−4.41	0.13	−0.20	−0.180	−0.150

3.4. Development of Inference Models and Taxon-Specific T July Optima

The T July models with all 98 lakes and all 143 chironomid taxa included in the analyses had coefficients of determination below 0.5 ($r^2_{boot} = 0.4–0.47$), an RMSEP = 1.49–1.75, and max biases $_{boot} = 2.78–3.92$ (Table 5, Figure 5A). The elimination of two outliers improved the statistical parameters of the model. For the 96 lakes and 143 chironomid taxa data set, the two-component WA-PLS model has an $r^2_{boot} = 0.60$ and RMSEP = 1.34 °C (Table 5, Figure 5B). The model tends to over-predict temperatures below 15 °C and under-predict temperatures above 15 °C.

Table 5. WA-PLS models for reconstructing mean July air temperature (T July). Root mean squared error for the training set (apparent RMSE); squared correlation between inferred and observed values(r^2); average bias in residuals (Av Bias); maximum bias in residuals (Max Bias); squared correlation between bootstrap predicted and observed values (r^2_{boot}); average bias in bootstrap residuals (Ave Bias $_{boot}$); maximum bias in bootstrap residuals (Max_Bias $_{boot}$); root mean squared error of prediction (RMSEP $_{boot}$); % reduction in RMSEP (% Change); and randomisation t-test significance (t-test).

WAPLS Component	RMSE	r^2	Av Bias	Max Bias	r^2_{boot}	Ave Bias $_{boot}$	Max_Bias $_{boot}$	RMSEP	% Change	t-Test
Full model (98 lakes. 143 taxa)										
1	1.113	0.68	0.005	1.344	0.45	−0.047	3.63	1.51
2	0.833	0.82	−0.044	0.857	0.49	−0.050	3.92	1.49	1.16	0.16
3	0.638	0.89	0.022	0.775	0.47	−0.052	3.27	1.59	−6.40	0.68
4	0.497	0.94	0.002	0.805	0.44	−0.037	2.90	1.68	−5.76	0.90
5	0.414	0.96	−0.005	0.654	0.43	−0.043	2.78	1.75	−3.92	0.98
Minus 2 lakes (96 lakes. 143 taxa)										
1	1.086	0.69	−0.005	1.647	0.58	−0.090	3.27	1.37
2	0.778	0.84	−0.040	0.722	0.60	−0.082	3.37	1.34	1.63	0.07
3	0.583	0.91	0.017	0.837	0.61	−0.097	2.66	1.38	−2.08	0.12
4	0.455	0.95	−0.003	0.648	0.60	−0.078	2.29	1.44	−4.17	0.81
5	0.374	0.96	−0.007	0.399	0.59	−0.077	2.18	1.48	−3.23	0.91

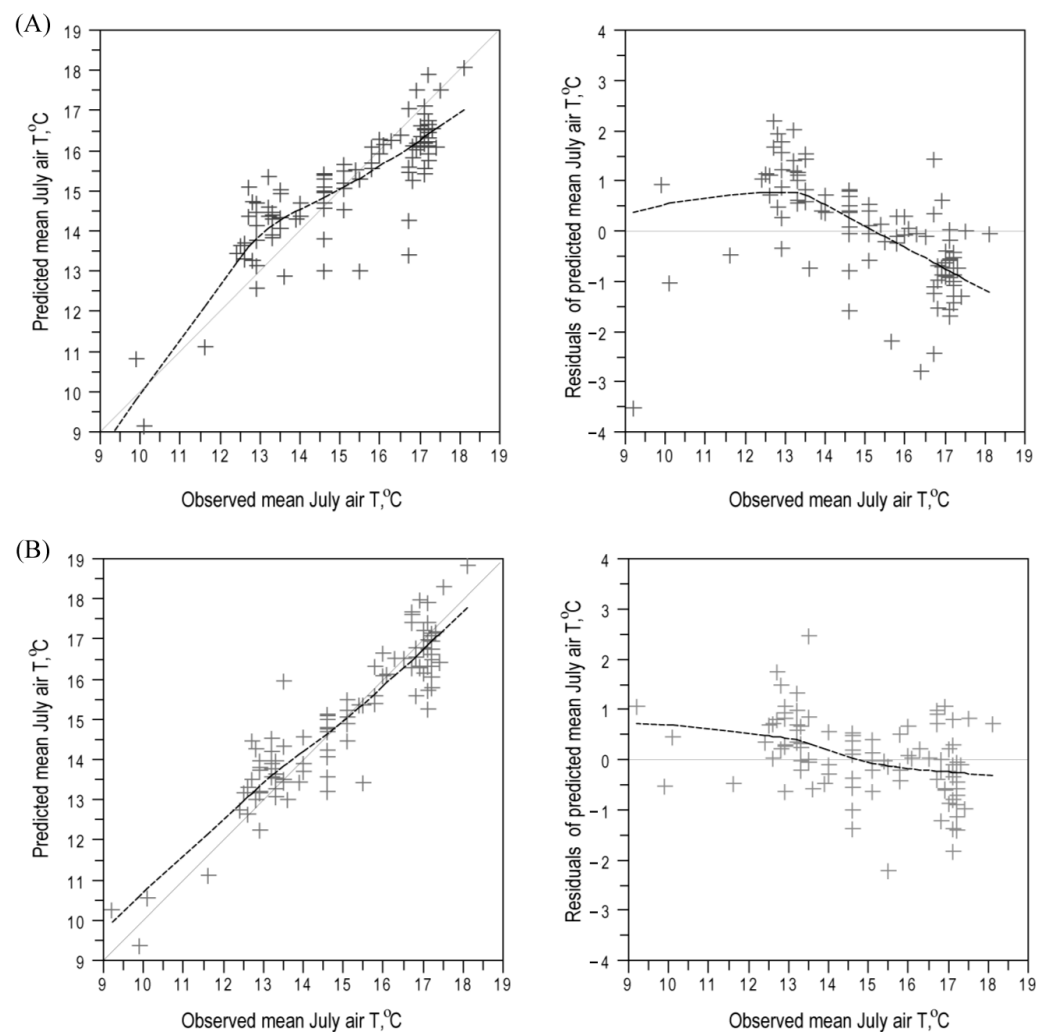


Figure 5. Observed vs. estimated T July and the residuals (inferred—observed) for (A) the full data set (98 lakes) chironomid-inferred mean July air temperatures 1—component WA-PLS model; (B) the 96 lakes NWE chironomid-inferred mean July air temperatures 2—component WA-PLS model. Trends in residuals are shown with a LOESS smoother (span = 0.45).

Of the 143 taxa, 61 have more than ten occurrences in the 96 lakes data set (apart from the undefined Chironomini, Tanytarsini, Orthocladiinae, Tanypodinae, and Chironomini larvula). All these 61 taxa have $N_2 \geq 5$, and their optima are likely to be reliably estimated [58] (Supplementary Electronic Material (SEM), Table S3). The T July optima for chironomid taxa in the data set ranged from 16.7 °C (*Microchironomus*), followed by *Tanytarsus lactescens*-type (16.6 °C) and *Chironomus plumosus*-type (16.4 °C), to 12.2 °C (*Corynocera oliveri*-type). Several taxa have T July optima below 12.2 °C, but they are rare in the data set. Test, using the generalized linear models showed that in the investigated dataset, 65.6% of the taxa with more than ten occurrences have a significant or highly significant relationship to T July (16.4% of the taxa have a highly significant relationship ($p \leq 0.001$) to T July).

4. Discussion

The new NWE dataset continues to our earlier studies on the influence of environmental factors on chironomid distribution and abundance in northern Eurasia. Our previous work included collecting taxonomic and ecological information on the lakes that are widely distributed across northern Eurasia [17–19,61–64]. The T July gradient presented in this manuscript from the NWE dataset (9.2 °C to 18.1 °C) is shorter than those in the WS (8.8–19 °C) and ES (3.4 to 18.8 °C) or NR (1.8 to 18.8 °C) and differs considerably from

the T range in the dataset from Kamchatka (1.8–13.3 °C) [16,19]. However, it demonstrates a similar or greater length when comparing the T July range in our study with the other datasets available for arctic regions of northern Eurasia (Sweden 7.0–14.7 °C, [12]; 11.3–17.1 °C, [14]; Norway 3.5–16 °C, [16]). The sampled range of temperatures in the NWE sufficiently reflects the modern ecological conditions in the region. Still, it shows some skewness in the distribution along the T July gradient, which can be seen as a task for our future investigation.

As in most chironomid-based datasets, the T July is the most significant explanatory variable in the NWE [65]. Though the DTL was not included in the original study [19], it was recently shown that DTL explain the highest proportion of variance in the north Russian dataset [19], while T July is the second important variable [65]. DTL is an important variable in the NWE, explaining a substantial proportion of the variance. Though T July and DTL appeared as non-biased parameters in the NWE, it was shown earlier that tree line position is related to climate in anthropogenically undisturbed areas [66–68]. However, DTL is a complex parameter that depends on different aspects of the climate, including T July. Therefore, even though the DTL can play an essential role in the chironomid distribution, from an ecological point of view it is more reasonable to perform reconstructions of direct parameters such as T July.

In the NWE, we investigated the chironomid fauna of the east European part of northern Eurasia using a palaeoecological approach. Although the taxonomic resolution of the palaeoecological study is lower than that of traditional hydrobiological or faunistic investigations [27], our findings revealed a high chironomid taxonomic richness in several new northern regions of Eurasia. The most widely distributed in the new data set taxa (*Psectrocladius sordidellus*-type, *Procladius*, *Cladotanytarsus mancus*-type, *Tanytarsus pallidicornis*-type, *Tanytarsus mendax*-type, *Sergentia coracina*-type, *Microtendipes pedellus*-type, *Dicrotendipes nervosus*-type, *Polypedilum nubeculosum*-type, *Cladopelma lateralis*-type, and *Tanytarsus lugens*-type) are identical to the most frequent taxa found in previously studied regions in Siberia, Kamchatka, and the Far East [19,44,69–73]. Due to the wide range of their environmental tolerances, these taxa have a cosmopolitan distribution [19]. Additionally, it may be that each morphotype comprises different species in different regions [27].

Fauna of the coldest lakes in the dataset (NZ and the Polar Urals) include several chironomid taxa that are also common in the coldest lakes of the Eastern regions of the Russian Arctic: *Hydrobaenus lugubris*-type, *Diplocladius*, and *Oliveridia*. However, *Orthocladus* type I and *Hydrobaenus conformis*-type, dominant in the coldest areas of Siberia, have only single occurrences in the NWE dataset. This is probably due to the limited number of lakes with a T July below 10 °C in the NWE, while these taxa dominate communities of lakes with a T July well below 10 °C in Siberia. Both taxa can probably be found more abundantly in the European part of Russia where the T July gradient of the NWE will be extended.

There are differences in the T July optima of the non-rare, common taxa between the available datasets. All T July optima in the NWE are higher than in Kamchatka [19]. The T July optima of 13 out of the 39 non-rare, common taxa for all datasets differ only within the calculated taxon-specific T July tolerances (SEM, Table S2). These are the most widespread taxa: *Procladius*, *Chironomus plumosus*-type, *Chironomus anthracinus*-type, *Cladopelma, lateralis*-type *Microtendipes pedellus*-type, *Polypedilum nubeculosum*-type, *Cladotanytarsus mancus*-type, *Corynocera ambigua*, *Paratanytarsus penicillatus*-type, *Tanytarsus mendax*-type, *Tanytarsus pallidicornis*-type, *Parakiefferiella bathophila*-type, and *Paraphaenocladus*.

The rest of the non-rare taxa demonstrate some distinction (Figure 6). For *Phaenopsectra flavipes*-type, *Micropsectra radialis*-type, *Heterotrissocladius maeeri*-type, and *Psectrocladius sordidellus*-type, the T July optima have intermediate values between the WS and ES. *Cricotopus laricomalis*-type, *Pseudochironomus*, *Parachironomus varus*-type, and *Dicrotendipes nervosus*-type have T July optima lower in the eastern datasets. For the rest of the taxa, the T July optima are higher in the NWE than in WS and ES datasets. Therefore, the presence of these taxa in sediment samples can substantially influence the reconstructed T July.

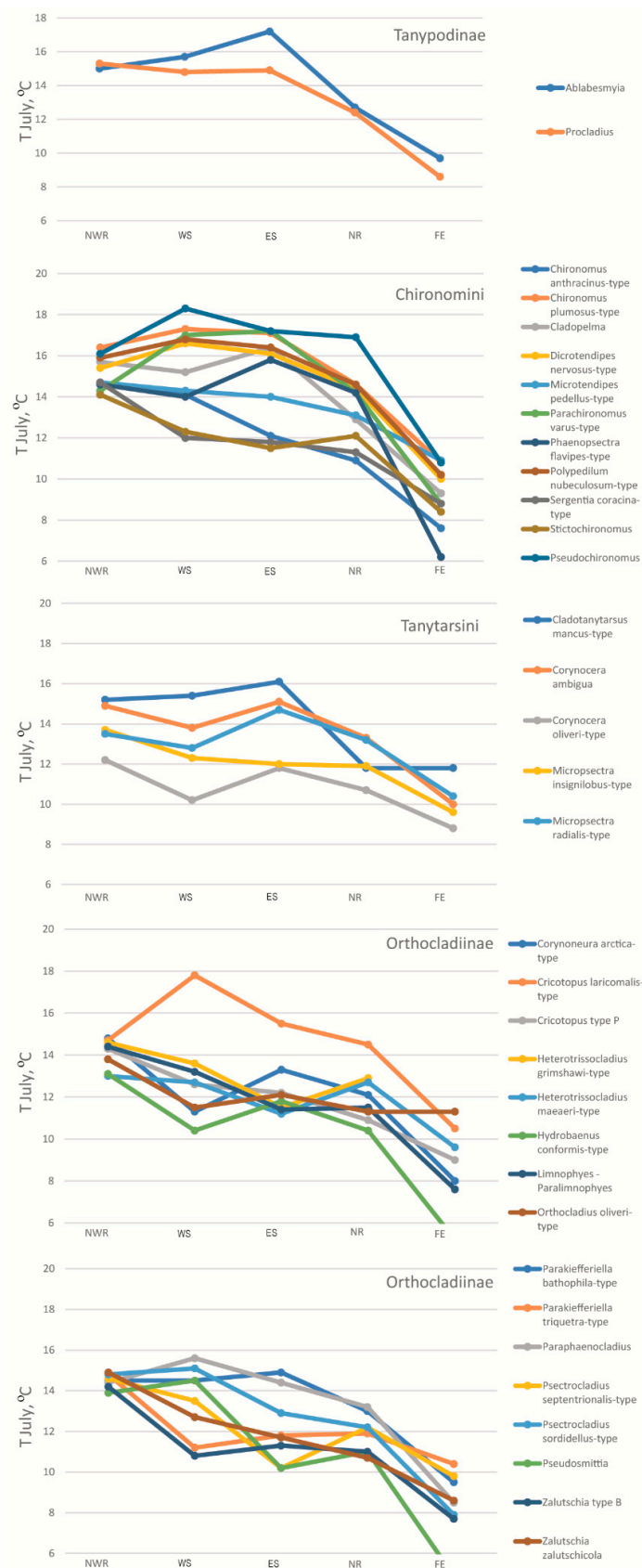


Figure 6. Mean July air T optima of non-rare taxa in northwest European (NWE), west Siberian (WS), east Siberian (ES), north Russian (NR) and Far East (FE) Russian models.

The most notable difference is observed for *Sergentia coracina*-type and *Stictochironomus*, known as cold stenotherm taxa [27,74,75]. In the new, they have T July optima of 14.7 °C and 14.1 °C, respectively (SEM, Table S3), which are approximately 3 °C higher than in the WS and ES. This is most likely due to the limited number of sites with a low T July in the NWE.

The revealed differences in the T optima of the non-rare chironomid taxa can play an essential role in the palaeoclimatic reconstructions if a non-regional dataset and an inference model are used.

The obtained chironomid-based, NWE mean July air temperature inference model has fairly moderate coefficients of determination and a good RMSEP when compared with other chironomid-based mean July air temperature inference models [12–16]. An earlier version of the NWE was used in palaeoclimatic reconstruction [29] and showed high sensitivity, revealing T July fluctuations during the Late Weichselian and Holocene in eastern Europe. Though improvements are still required in order to reach better transfer function parameters, the NWE model can be applied for palaeoclimatic reconstructions in most northern and northwestern Eurasia.

5. Conclusions

We compiled an NWE calibration set from seven new northwest European and two previously investigated northeast European regions of arctic and sub-arctic Russia.

The mean July air temperature is the most important explanatory variable in the NWE. The sampled range of temperatures in the NWE sufficiently reflects the current ecological conditions in the region; however, cold areas are under-represented in the dataset.

The most widely distributed chironomid taxa in the NWE data set are identical to the dominant taxa found in previously studied regions in Siberia and Kamchatka. The T July optima of the taxa that are dominant in all north Russian datasets (NWE, west Siberian, east Siberian, and north Russian) differ only within the ranges of calculated, taxon-specific T July tolerances. They are higher than the T July optima of these taxa in the Kamchatka regional dataset.

The T optima of the other non-rare chironomid taxa demonstrate some distinction. The revealed differences in the T optima of the non-rare chironomid taxa can play an essential role in palaeoclimatic reconstructions if a non-regional dataset and inference model are used.

The obtained NWE chironomid-based mean July air temperature inference model has solid statistical parameters ($r^2 = 0.84$; $r^2_{boot} = 0.60$; $RMSEP_{boot} = 1.34^\circ\text{C}$) and can be applied for palaeoclimatic reconstructions in most parts of the northern and northwestern Eurasia.

Supplementary Materials: The following supporting information can be downloaded at: <https://www.mdpi.com/article/10.3390/w15050976/s1>. Table S1: Summary of the environmental data for the regions of investigations. WD for water depth; Table S2: Eigenvalues. Cumulative % variance and significance of the CCA axes; Table S3: Number of occurrences (N), maximum abundance (Max), N2, response to T July (WS model: HOF model; NWE, ES, FM, NR, and FE models: Resp, value for significance of the relationship with the T July based on generalized linear response model, set to a quadratic degree and Poisson distribution $p < 0.05$: - not significant; significant, small x; highly significant, $p < 0.001$, capital X), and WA optima (Opt) and tolerances (tol) for taxa with more than 10 occurrences in data-sets. HOF model I shows no response to July air temperature; II shows a sigmoidal increasing or decreasing response; III shows a response which reaches a plateau; IV shows a unimodal response; and V shows a skewed, unimodal response. Data sets: NWE—northwest European Russia, WS—west Siberian, ES—east Siberian, FM—full model, NR—north Russian, FE—Far East.

Author Contributions: L.N., conceptualization, methodology, software, formal analysis, and writing—original draft preparation; L.S., field data collection and chironomid analysis; T.S., field work organization and sample collection; I.G., tree line information and visualization; A.B.K. and N.S., field work organization and sample collection. All authors have read and agreed to the published version of the manuscript.

Funding: The data presented in this paper have been collected and treated for more than five years and we acknowledge all funds and organizations that supported the authors during this period. The numerical analysis was performed in the frame of the RSF no. 20-17-00135; The contribution by L.S. and I.G. were supported by the Ministry of Education of the Russian Federation as part of a state task (project No. VRFY-2023-0010); the chironomid analyses was funded by the RSF project 22-17-00113; and T.S. was supported the State Research Program of the Institute of Limnology RAS—SPC RAS No. 0154-2019-0001.

Data Availability Statement: The original data, including lake coordinates, will be available in the PANGEA database upon the manuscript acceptance.

Acknowledgments: The authors would like to acknowledge all Russian colleagues who helped with collecting the samples during the field work. Special thanks to Yuri Mazei and Andrey Tsyganov for their help in organizing the expedition to Karelian Isthmus. We thank employees of the Laboratory of paleolimnology and Laboratory of Geology and Metallogeny for the newest deposits of Karelian SC RAS for their help in collecting sediment samples for chironomid analysis. A.K. would like to express his appreciation to the Open Ocean project and its scientific leader, Maria Gavrilov, for the opportunity to participate in the O2A2-2015 expedition and collect samples on Novaya Zemlya. We are grateful to the reviewers of the manuscript for their significant comments and improvements.

Conflicts of Interest: The authors declare no conflict of interest. The funders had no role in the design of the study; in the collection, analyses, or interpretation of data; in the writing of the manuscript; or in the decision to publish the results.

References

1. Coffman, W.; Ferrington, L. *Chironomidae*; Merritt, R., Cummins, K., Eds.; Kendall/Hunt Publishing Company: Dubuque, IA, USA, 1996.
2. Stief, P.; Nazarova, L.; de Beer, D. Chimney construction by *Chironomus riparius* larvae in response to hypoxia: Microbial implications for freshwater sediments. *J. N. Am. Benthol. Soc.* **2005**, *24*, 858–871. [[CrossRef](#)]
3. Hölker, F.; Vanni, M.J.; Kuiper, J.J.; Meile, C.; Grossart, H.-P.; Stief, P.; Adrian, R.; Lorke, A.; Dellwig, O.; Brand, A.; et al. Tube-dwelling invertebrates: Tiny ecosystem engineers have large effects in lake ecosystems. *Ecol. Monogr.* **2015**, *85*, 333–351. [[CrossRef](#)]
4. Engels, S.; Medeiros, A.S.; Axford, Y.; Brooks, S.J.; Heiri, O.; Luoto, T.P.; Nazarova, L.; Porinchu, D.F.; Quinlan, R.; Self, A.E. Temperature change as a driver of spatial patterns and long-term trends in chironomid (Insecta: Diptera) diversity. *Glob. Chang. Biol.* **2020**, *26*, 1155–1169. [[CrossRef](#)] [[PubMed](#)]
5. Brooks, S.J. Fossil midges (Diptera: Chironomidae) as palaeoclimatic indicators for the Eurasian region. *Quat. Sci. Rev.* **2006**, *25*, 1894–1910. [[CrossRef](#)]
6. Medeiros, A.S.; Quinlan, R.; Sprules, G. The distribution of the Chironomidae (Insecta: Diptera) along multiple environmental gradients in lakes and ponds of the eastern Canadian Arctic. *Can. J. Fish. Aquat. Sci.* **2011**, *68*, 1511–1527. [[CrossRef](#)]
7. Eggermont, H.; Heiri, O. The chironomid-temperature relationship: Expression in nature and palaeoenvironmental implications. *Biol. Rev. Camb. Philos. Soc.* **2012**, *87*, 430–456. [[CrossRef](#)] [[PubMed](#)]
8. Fortin, M.-C.; Medeiros, A.S.; Gajewski, K.; Barley, E.M.; Larocque-Tobler, I.; Porinchu, D.F.; Wilson, S.E. Chironomid-environment relations in northern North America. *J. Paleolimnol.* **2015**, *54*, 223–237. [[CrossRef](#)]
9. Barley, E.M.; Walker, I.R.; Kurek, J.; Cwynar, L.C.; Mathewes, R.W.; Gajewski, K.; Finney, B.P. A northwest North American training set: Distribution of freshwater midges in relation to air temperature and lake depth. *J. Paleolimnol.* **2006**, *36*, 295–314. [[CrossRef](#)]
10. Dieffenbacher-Krall, A.; Vandergoes, M.J.; Denton, G.H. An inference model for mean summer air temperatures in the Southern Alps, New Zealand, using subfossil chironomids. *Quat. Sci. Rev.* **2007**, *26*, 2487–2504. [[CrossRef](#)]
11. Rees, A.B.H.; Cwynar, L.C.; Cranston, P. Midges (Chironomidae, Ceratopogonidae, Choaboridae) as a temperature proxy: A training set from Tasmania, Australia. *J. Paleolimnol.* **2008**, *40*, 1159–1178. [[CrossRef](#)]
12. Larocque, I.; Hall, R.; Grahn, E. Chironomids as indicators of climate change: A 100-lake training set from a subarctic region of northern Sweden (Lapland). *J. Paleolimnol.* **2001**, *26*, 307–322. [[CrossRef](#)]
13. Heiri, O.; Lotter, A.F.; Hausmann, S.; Kienast, F. A chironomid-based Holocene summer air temperature reconstruction from the Swiss Alps. *Holocene* **2003**, *13*, 477–484. [[CrossRef](#)]
14. Luoto, T.P. Subfossil Chironomidae (Insecta: Diptera) along a latitudinal gradient in Finland: Development of a new temperature inference model. *J. Quat. Sci.* **2009**, *24*, 150–158. [[CrossRef](#)]
15. Luoto, T.; Kotrys, B.; Płóciennik, M. East European chironomid-based calibration model for past summer temperature reconstructions. *Clim. Res.* **2018**, *77*, 63–76. [[CrossRef](#)]

16. Self, A.; Brooks, S.; Birks, H.; Nazarova, L.; Porinchu, D.; Odland, A.; Yang, H.; Jones, V. The distribution and abundance of chironomids in high-latitude Eurasian lakes with respect to temperature and continentality: Development and application of new chironomid-based climate-inference models in northern Russia. *Quat. Sci. Rev.* **2011**, *30*, 1122–1141. [[CrossRef](#)]
17. Nazarova, L.B.; Pestryakova, L.A.; Ushnitskaya, L.A.; Hubberten, H.-W. Chironomids (Diptera: Chironomidae) in lakes of central Yakutia and their indicative potential for paleoclimatic research. *Contemp. Probl. Ecol.* **2008**, *1*, 335–345. [[CrossRef](#)]
18. Nazarova, L.; Herzschuh, U.; Wetterich, S.; Kumke, T.; Pestryakova, L. Chironomid-based inference models for estimating mean July air temperature and water depth from lakes in Yakutia, northeastern Russia. *J. Paleolimnol.* **2011**, *45*, 57–71. [[CrossRef](#)]
19. Nazarova, L.; Self, A.E.; Brooks, S.J.; van Hardenbroek, M.; Herzschuh, U.; Diekmann, B. Northern Russian chironomid-based modern summer temperature data set and inference models. *Glob. Planet. Chang.* **2015**, *134*, 10–25. [[CrossRef](#)]
20. Nazarova, L.B.; Sapelko, T.V.; Kuznetsov, D.D.; Syrykh, L.S. Palaeoecological and Palaeoclimatical Reconstructions of Holocene According Chironomid Analysis of Lake Glubokoye Sediments. *Dokl. Biol. Sci.* **2015**, *460*, 57–60. [[CrossRef](#)]
21. Subetto, D.A.; Nazarova, L.B.; Pestryakova, L.A.; Syrykh, L.S.; Andronikov, A.V.; Biskaborn, B.; Diekmann, B.; Kuznetsov, D.D.; Sapelko, T.V.; Grekov, I.M. Paleolimnological studies in Russian northern Eurasia: A review. *Contemp. Probl. Ecol.* **2017**, *4*, 327–335. [[CrossRef](#)]
22. Syrykh, L.; Subetto, D.; Nazarova, L. Paleolimnological studies on the East European Plain and nearby regions: The PaleoLake Database. *J. Paleolimnol.* **2021**, *65*, 369–375. [[CrossRef](#)]
23. Solovieva, N.; Jones, V.J.; Nazarova, L.; Brooks, S.J.; Birks, H.J.B.; Grytnes, J.-A.; Appleby, P.G.; Kauppila, T.; Kondratenok, B.; Renberg, I.; et al. Paleolimnological Evidence for Recent Climate Change in Lakes from the Northern Urals, Russia. *J. Paleolimnol.* **2005**, *33*, 463–482. [[CrossRef](#)]
24. Nazarova, L.B.; Self, A.E.; Brooks, S.J.; Solovieva, N.; Syrykh, L.S.; Dauvalter, V.A. Chironomid fauna of the lakes from the Pechora river basin (east of European part of Russian Arctic): Ecology and reconstruction of recent ecological changes in the region. *Contemp. Probl. Ecol.* **2017**, *4*, 350–362. [[CrossRef](#)]
25. Nazarova, L.B.; Frolova, L.A.; Palagushkina, O.V.; Rudaya, N.A.; Syrykh, L.S.; Grekov, I.M.; Solovieva, N.; Loskutova, O.A. Recent shift in biological communities: A case study from the Eastern European Russian Arctic (Bol'shezemelskaya Tundra). *Polar Biol.* **2021**, *44*, 1107–1125. [[CrossRef](#)]
26. Andreev, A.; Tarasov, P.; Schwamborn, G.; Iljashuk, B.; Iljashuk, E.; Bobrov, A.; Klimanov, V.; Rachold, V. Holocene palaeoenvironmental records from Nikolay Lake, Lena Delta, Arctic Russia. *Palaeogeogr. Palaeoclim. Palaeoecol.* **2004**, *209*, 197–217. [[CrossRef](#)]
27. Brooks, S.J.; Langdon, P.G.; Heiri, O. *Using and Identifying Chironomid Larvae in Palaeoecology*; QRA Technical Guide No 10; Quaternary Research Association: London, UK, 2007.
28. Pliik, A.; Engels, S.; Luoto, T.P.; Nazarova, L.; Salonen, J.S.; Helmens, K.F. Chironomid-based temperature reconstruction for the Eemian Interglacial (MIS 5e) at Sokli, northeast Finland. *J. Paleolimnol.* **2019**, *61*, 355–371. [[CrossRef](#)]
29. Płóciennik, M.; Mroczkowska, A.; Pawłowski, D.; Wieckowska-Lüth, M.; Kurzawska, A.; Rzodkiewicz, M.; Okupny, D.; Szymańda, J.; Mazurkevich, A.; Dolbunova, E.; et al. Summer temperature drives the lake ecosystem during the Late Weichselian and Holocene in Eastern Europe: A case study from East European Plain. *Catena* **2022**, *214*, 106206. [[CrossRef](#)]
30. Renberg, I. The HON-Kajak sediment corer. *J. Paleolimnol.* **1991**, *6*, 167–170. [[CrossRef](#)]
31. New, M.; Lister, D.; Hulme, M.; Makin, I. A high-resolution data set of surface climate over global land areas. *Clim. Res.* **2002**, *21*, 1–25. [[CrossRef](#)]
32. Overland, J.E.; Wang, M. The Arctic Climate Paradox: The Recent Decrease of the Arctic Oscillation. *Geophys. Res. Lett.* **2005**, *32*, L06701. [[CrossRef](#)]
33. Brown, J.; Ferrians, O.J., Jr.; Heginbottom, J.A.; Melnikov, E.S. *Circum-Arctic Map of Permafrost and Ground Ice Conditions*; National Snow and Ice Data Center/World Data Center for Glaciology; Digital Media: Boulder, CO, USA, 1998. [[CrossRef](#)]
34. Esri, R. *ArcGIS Desktop: Release 10.6*; Environmental Systems Research Institute: Redlands, CA, USA, 2011.
35. Wiederholm, T. Chironomidae of the Holarctic region. Keys and diagnoses. Part 1. Larvae. *Entomol. Scand.* **1983**, *9* (Suppl. S19), 1–457.
36. Heiri, O.; Lotter, A.F. Effect of low count sums on quantitative environmental reconstructions: An example using subfossil chironomids. *J. Paleolimnol.* **2001**, *26*, 343–350. [[CrossRef](#)]
37. Quinlan, R.; Smol, J. Setting minimum head capsule abundance and taxa deletion criteria in chironomid-based inference models. *J. Paleolimnol.* **2001**, *26*, 327–342. [[CrossRef](#)]
38. Biskaborn, B.K.; Nazarova, L.; Pestryakova, L.A.; Syrykh, L.; Funck, K.; Meyer, H.; Chaplugin, B.; Vyse, S.; Gorodnichev, R.; Zakharov, E.; et al. Spatial distribution of environmental indicators in surface sediments of Lake Bolshoe Toko. *Biogeosciences* **2019**, *16*, 4023–4049. [[CrossRef](#)]
39. Kumke, T.; Ksenofontova, M.; Pestryakova, L.; Nazarova, L.; Hubberten, H.-W. Limnological characteristics of lakes in the lowlands of Central Yakutia, Russia. *J. Limnol.* **2007**, *66*, 40–53. [[CrossRef](#)]
40. Sokal, R.R.; Rohlf, F.J. *Biometry: The Principles and Practice of Statistics in Biological Research*; W. H. Freeman and Co.: New York, NY, USA, 1995.
41. Palagushkina, O.V.; Nazarova, L.B.; Wetterich, S.; Schirrmeister, L. Diatoms of modern bottom sediments in Siberian arctic. *Contemp. Probl. Ecol.* **2012**, *5*, 413–422. [[CrossRef](#)]

42. Lepš, J.; Šmilauer, P. *Multivariate Analysis of Ecological Data Using CANOCO*; Cambridge University Press: New York, NY, USA, 2003.
43. Birks, H.J.B. Quantitative Palaeoenvironmental Reconstructions. In *Statistical Modelling of Quaternary Science Data*; Technical guide 5; Quaternary Research Association: Cambridge, UK, 1995; pp. 161–254.
44. Nazarova, L.; Bleibtreu, A.; Hoff, U.; Dirksen, V.; Diekmann, B. Changes in temperature and water depth of a small mountain lake during the past 3000 years in Central Kamchatka reflected by a chironomid record. *Quat. Int.* **2017**, *447*, 46–58. [[CrossRef](#)]
45. ter Braak, C.J.F. *Ordination*; Jongman, R.H.G., ter Braak, C.J.F., Tongeren, O.F.R., Eds.; Cambridge University Press: Cambridge, UK, 1995.
46. Šmilauer, P.; Lepš, J. *Multivariate Analysis of Ecological Data using CANOCO 5*; Cambridge University Press: Cambridge, UK, 2014.
47. ter Braak, C.J.F. *Update Notes: CANOCO Version 3.10*; Agricultural Mathematics Group: Wageningen, The Netherlands, 1990.
48. ter Braak, C.J.F.; Šmilauer, P. *CANOCO for Windows: Software for Community Ordination (Version 4.5)*; Microcomputer Power: Ithaca, NY, USA, 2002.
49. Gavin, D.G.; Oswald, W.; Wahl, E.R.; Williams, J.W. A statistical approach to evaluating distance metrics and analog assignments for pollen records. *Quat. Res.* **2003**, *60*, 356–367. [[CrossRef](#)]
50. Hammer, Ø.; Harper, D.A.T.; Raan, P.D. PAST: Palaeontological statistics software package for education and data analysis. *Palaeontol. Electron.* **2001**, *41*, 9.
51. Dowsett, H.J.; Robinson, M.M. Application of the modern analogue technique (MAT) of sea surface temperature estimation to middle Pliocene North Pacific planktic foraminifer assemblages. *Palaeontol. Electron.* **1998**, *1*, 22.
52. ter Braak, C.J.F.; Looman, C.W.N. Weighted Averaging, Logistic Regression and the Gaussian Response Model. *Vegetatio* **1986**, *65*, 3–11. [[CrossRef](#)]
53. ter Braak, C.J.F.; Juggins, S. Weighted Averaging Partial Least Squares Regression (WA-PLS): An Improved Method for Reconstructing Environmental Variables from Species Assemblages. *Hydrobiologia* **1993**, *269–270*, 485–502. [[CrossRef](#)]
54. Altman, D.G.; Bland, J.M. Measurement in Medicine: The Analysis of Method Comparison Studies. *Statistician* **1983**, *32*, 307–317. [[CrossRef](#)]
55. Birks, H.J.B. Numerical tools in paleolimnology progress, potential, and problems. *J Paleolimnol.* **1998**, *20*, 307–332. [[CrossRef](#)]
56. Birks, H.J.B.; Juggins, S.; Line, J.M. *Lake Surface-Water Chemistry Reconstructions from Paleolimnological Data*; Mason, B., Ed.; Cambridge University Press: Cambridge, UK, 1990.
57. Birks, H.J.B.; Line, J.M.; Juggins, S.; Stevenson, A.C.; ter Braak, C.J.F. Diatoms and pH Reconstruction. *Philos. Trans. R. Soc. B* **1990**, *327*, 263–278.
58. Brooks, S.J.; Birks, H.J.B. Chironomid-Inferred Air Temperatures from Late-Glacial and Holocene Sites in North-West Europe: Progress and Problems. *Quat. Sci. Rev.* **2001**, *20*, 1723–1741. [[CrossRef](#)]
59. Juggins, S. *C2 Version 1.5 User Guide. Software for Ecological and Palaeoecological Data Analysis and Visualisation*; Newcastle University: Newcastle upon Tyne, UK, 2007.
60. Juggins, S. Quantitative Reconstructions in Paleolimnology: New Paradigm or Sick Science? *Quat. Sci. Rev.* **2013**, *64*, 20–32. [[CrossRef](#)]
61. Syrykh, L.S.; Nazarova, L.B.; Herzsuh, U.; Subetto, D.A.; Grekov, I.M. Reconstruction of palaeoecological and palaeoclimatic conditions of the Holocene in the south of the Taimyr according to an analysis of lake sediments. *Contemp. Probl. Ecol.* **2017**, *4*, 363–369. [[CrossRef](#)]
62. Nazarova, L.; Grebennikova, T.A.; Razjigaeva, N.G.; Ganzey, L.A.; Belyanina, N.I.; Arslanov, K.A.; Kaistrenko, V.M.; Gorbunov, A.O.; Kharlamov, A.A.; Rudaya, N.; et al. Reconstruction of Holocene environmental changes in Southern Kurils (North-Western Pacific) based on palaeolake sediment proxies from Shikotan Island. *Glob. Planet. Chang.* **2017**, *159*, 25–36. [[CrossRef](#)]
63. Nazarova, L.; Syrykh, L.S.; Mayfield, R.J.; Frolova, L.A.; Ibragimova, A.G.; Grekov, I.M.; Subetto, D.A. Palaeoecological and palaeoclimatic conditions on the Karelian Isthmus (northwestern Russia) during the Holocene: Multi-Proxy Analysis of Sediments from the Lake Medvedevskoe. *Quat. Res.* **2020**, *95*, 65–83. [[CrossRef](#)]
64. Druzhinina, O.; Kublitskii, J.; Nazarova, L.; Subetto, D.; Syrykh, L.; Arslanov, K.; Stančikaitė, M.; Vaikutienė, G.; Kul'kova, M. Palaeoenvironmental Conditions in South-Eastern Part of the Baltic Region during the Late Pleistocene—Holocene Transition (Kaliningrad District, Russia). *Boreas* **2020**, *49*, 544–561. [[CrossRef](#)]
65. Mayfield, R.J.; Langdon, P.G.; Doncaster, C.P.; Dearing, J.A.; Wang, R.; Nazarova, L.B.; Medeiros, A.S.; Brooks, S.J. Metrics of structural change as indicators of chironomid community stability in high latitude lakes. *Quat. Sci. Rev.* **2020**, *249*, 106594. [[CrossRef](#)]
66. MacDonald, G.M.; Szeicz, J.M.; Claricoates, J.; Dale, K.A. Response of the Central Canadian Treeline to Recent Climatic Changes. *Ann. Assoc. Am. Geogr.* **1998**, *88*, 183–208. [[CrossRef](#)]
67. Macdonald, G.M.; Velichko, A.A.; Kremenetski, C.V.; Borisova, O.K.; Goleva, A.A.; Andreev, A.; Cwynar, L.C.; Riding, R.T.; Forman, S.; Edwards, T.W.; et al. Holocene Treeline History and Climate Change Across Northern Eurasia. *Quat. Res.* **2000**, *53*, 302–311. [[CrossRef](#)]
68. Harsch, M.A.; Bader, M. Treeline form—A potential key to understanding treeline dynamics. *Glob. Ecol. Biogeogr.* **2011**, *20*, 582–596. [[CrossRef](#)]

69. Self, A.; Klimaschewski, A.; Solovieva, N.; Jones, V.; Andrén, E.; Andreev, A.; Hammarlund, D.; Brooks, S. The relative influences of climate and volcanic activity on Holocene lake development inferred from a mountain lake in central Kamchatka. *Glob. Planet. Chang.* **2015**, *134*, 67–81. [[CrossRef](#)]
70. Wetterich, S.; Schirrmeyer, L.; Nazarova, L.; Palagushkina, O.; Bobrov, A.; Pogosyan, L.; Savelieva, L.; Syrykh, L.; Matthes, H.; Fritz, M.; et al. Holocene thermokarst and pingo development in the Kolyma Lowland (NE Siberia). *Permafrost. Periglac.* **2018**, *29*, 182–198. [[CrossRef](#)]
71. Porinchu, D.F.; Cwynar, L.S. Late-Quaternary History of Midge Communities and Climate from a Tundra Site near the Lower Lena River, Northeast Siberia. *J. Paleolimnol.* **2002**, *27*, 59–69. [[CrossRef](#)]
72. Nazarova, L.; Sachse, D.; Fuchs, H.G.E.; Dirksen, V.; Dirksen, O.; Syrykh, L.; Razjigaeva, N.G.; Rach, O.; Diekmann, B. Holocene evolution of a proglacial lake in southern Kamchatka, Russian Far East. *Boreas* **2021**, *50*, 1011–1026. [[CrossRef](#)]
73. Brodin, Y.W. The Postglacial History of Lake Flarken, Southern Sweden, Interpreted from Subfossil Insect Remains. *Int. Rev. Gesamten Hydrobiol. Hydrogr.* **1986**, *71*, 371–432. [[CrossRef](#)]
74. Brundin, L. Zur Systematic Der Orthocladiinae (Dipt., Chironomidae) Report of the Institute of Freshwater Research. *Drottningholm* **1956**, *37*, 5–186.
75. Quinlan, R.; Smol, J.P.; Hall, R.I. Quantitative Inferences of Past Hypolimnetic Anoxia in South-Central Ontario Lakes using Fossil Midges (Diptera: Chironomidae). *Can. J. Fish. Aquat. Sci.* **1998**, *55*, 587–596. [[CrossRef](#)]

Disclaimer/Publisher’s Note: The statements, opinions and data contained in all publications are solely those of the individual author(s) and contributor(s) and not of MDPI and/or the editor(s). MDPI and/or the editor(s) disclaim responsibility for any injury to people or property resulting from any ideas, methods, instructions or products referred to in the content.